AN INTELLIGENT GUIDE FOR CLOSE RANGE PHOTOGRAMMETRY

Matthieu Bach, M.Sc. Student
Sylvie Daniel, Director
Geomatics Department
Pavillon Louis-Jacques Casault, Local 1170
Université Laval
Quebec, QC, Canada, G1V 0A6
matthieu.bach.1@ulaval.ca
Sylvie.Daniel@scg.ulaval.ca

ABSTRACT

This paper proposes a new tool for close range photogrammetry survey. It has been designed to assist non-expert users when conducting 3D survey of infrastructures. Close range photogrammetry requires specific acquisition setup in order to build precise and accurate 3D model. While an expert user will know where to locate his camera stations and how to overcome terrain hindrance in order to still comply with his precision requirement, a non-expert user may be clueless. The proposed guide aims at informing the user about his current acquisition choices and their impacts on the resulting 3D model. The paper presents the solution we designed and the various components it includes. Some results are also provided.

INTRODUCTION

Aging infrastructures are turning into a major concern for the Canadian public maintenance services. Recent newspaper headlines recounting accidents in relation to bridge and underground parking lot failures sent a strong warning to the responsible authority. Thus, assessing and monitoring the infrastructures has become a priority for the public security sake.

Among the 3D modeling techniques available for infrastructure monitoring, close range photogrammetry is often used since its principles are well known and have sound mathematical bases (Remondino et al., 2006). In addition, this is a reliable and relatively affordable technique, and a lot of photogrammetric processes have been developed for quick and precise 3D measurement (a 1/20mm precision can be reached with special techniques as proved by the V-Star system (Brown, 1997)). The main drawback of close range photogrammetry is the level of expertise required to build precise and accurate 3D models. Technicians from maintenance service companies are generally not acquainted with photogrammetry techniques. Therefore they cannot use the current available expert-oriented solutions to get 3D models and measurements fulfilling civil engineering requirements. A solution is required to provide non-expert users with relevant photogrammetric tools to survey infrastructures. The design of such solution is the focus of our current research project.

A photogrammetric project can generally be broken up into 3 successive steps:

1. Project planning or photogrammetric network design
2. On site data acquisition
3. Image processing towards 3D modeling

On site data acquisition is a crucial step since it will greatly influence the system capacity to build an accurate 3D model. The network design step aims at identifying the optimum acquisition configuration to fulfill the accuracy requirements. As an example, the network design step will specify the number of acquisition stations, their location, the most relevant camera focal length etc. Therefore, when going on site, the user has to follow these specifications. While an expert user will know where to locate his camera stations and how to overcome terrain hindrance in order to still comply with the network specifications, a non-expert user may be clueless. He will have no information about his current acquisition choices and their impacts on the resulting 3D model. Providing photogrammetric solutions to non-experts in photogrammetry has been a problem tackled in various application contexts. In each of these contexts, researchers have emphasized the problems induced by users' inexperience. For example, Drap et al. (Drap, 2001) designed a tool to help selecting homologous points on images relying on a correlation algorithm. Chandler (Chandler, 1999), provides some recommendations for non-expert users to create Digital Elevation Models (DEM) from stereo images. Marzolff and Poesen (Marzolff, 2009) found that those users are not aware that the image resolution is not the same as the DEM resolution. Walker and Willgoose (Walker, 1999) underlined that geomorphology professionals, among others, are not fully aware of the restrictions of DEMs as sources of spatial information. All these examples tends to prove that inexperienced users don't have clearly in mind that the images used as a source of information are a key point in their photogrammetric process, that the quality of the final result depends directly on the good performance of the acquisition process.

This paper will describe the solution we designed and developed in order to fulfill the need for guidelines and feedbacks during the acquisition process. This solution specifically target non-expert user of photogrammetry technologies. The first part of the paper will provide an overview of our solution, including a description of the interface, and the embedded simulator. Then the second part of the paper will be dedicated to the solution performances and the outcome of tests we conducted with a group of users. Finally the last part of the paper will provide some conclusion and perspective about this work.

OVERVIEW OF THE SOLUTION

As mentioned in the introduction paragraph, the first stage of the photogrammetric survey consists in designing the network. The network specifications will ensure the acquisition configuration yields to 3D model fulfilling the monitoring precision requirements. The goal of the proposed solution is to assist non-expert user through the onsite photographs acquisition process while relying on the network specifications. In the current context of infrastructure monitoring, it can be assumed that a first survey has already been done, and, consequently, a 3D model of the object is available and can be exploited by the proposed solution.

The proposed solution consists mainly of two components:

- A graphical interface: its purpose is to guide the user through the acquisition process (Figure 1)
- A simulator: it aims at providing the user with information about the camera positions in relation to the ideal positions specified by the network design stage.

These two components will be described in the following paragraphs.

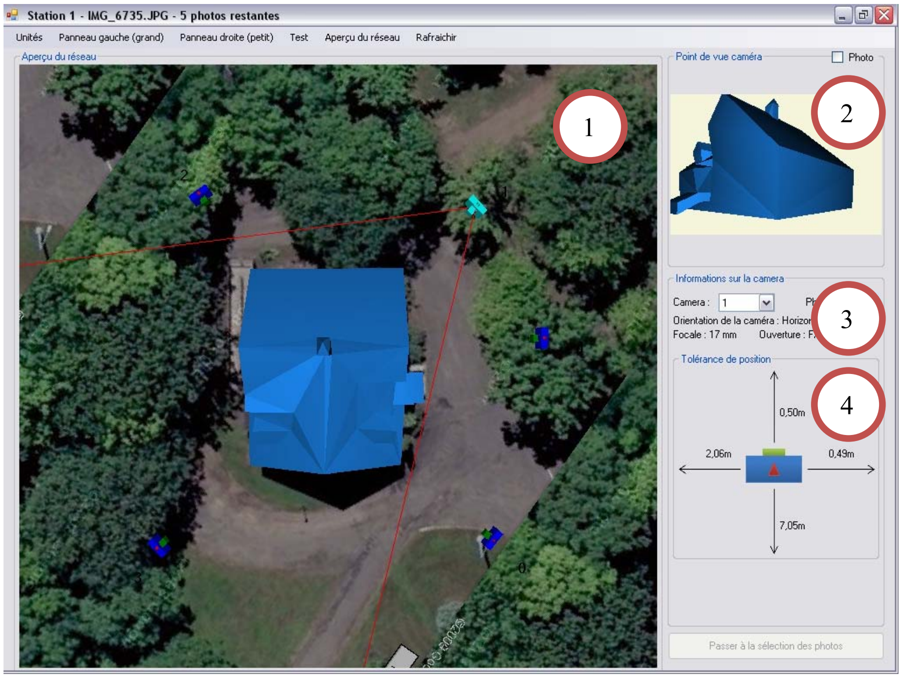
Station 1 - IMG_6735.JPG - 5 photos restantes

Camera : 1

Orientation de la caméra : Horizon

Focale : 17 mm   Ouverture : F

Figure 1. Interface of the application.

DESCRIPTION OF THE INTERFACE

The interface consists mainly of four display areas. Each of them provides the user with complementary view or information about the acquisition context. The contents and goal of each area is the following:

- **Area 1 (Figure 1):** This area provides an overview of the acquisition site, of the network and of the 3D model. The visualization of the acquisition site relies on a map or satellite view exported from Google Maps. The 3D model of the infrastructure to monitor is positioned on this view at its corresponding location. In the proposed example (i.e. Figure 1), the 3D model, a house, is displayed in light blue in the center of the area. The positions where the photographs should be taken as specified by the network are represented on the map/satellite view by dark blue cameras. When clicking on a camera, information about its configuration and its viewpoint on the model becomes available on the right hand side of the interface. The currently selected camera is displayed in cyan and its field of view is bounded by two lines (in red in the proposed example). The location of these lines is computed based on the camera focal length. The user can fully interact with this overview of the acquisition site to get a better point of view if needed. He can especially zoom and rotate the whole view in 3D. When zooming in the view, additional information can be displayed allowing a precise positioning of the camera station. Thus, the user can get information about the theoretical distance between the camera and various points of the model (cf. Area 5 on Figure 2). These distances are computed based on the camera location specified by the network.
- **Area 2 (Figure 1):** This display area provides the user with a view of the 3D model according to the viewpoint of the currently selected camera. In other words, the user can know what the infrastructure should look like if he/she was looking at it from the same location and orientation as the camera. Instead of the 3D model, picture acquired from the camera station during a previous survey can also be displayed to the user (cf. Area 6 on Figure 2). Relying on this display, the user can try to get the same photo and adjust the settings and configuration accordingly.
- **Area 3 (Figure 1):** This display area provides the camera setup. Information consists of the focal length and the camera orientation. The latter consists of the roll, pitch and yaw angles. The roll angle specifies if the camera is handled horizontally or vertically, namely if a portrait or landscape format picture is taken. The yaw and pitch angles are defined according to the point at which the camera is aiming (cf. Area 2).
- **Area 4 (Figure 1):** This display area provides the "tolerances" in relation to the camera positions as specified by the network. In other words, the user can know the maximum distance from the ideal camera station the picture can be taken without impacting the subsequent 3D modeling accuracy and precision. The tolerances are expressed as distances along four directions: in front, behind, on the left, on the right of the camera. The tolerances are computed by the solution simulator as it will be detailed in the next section.

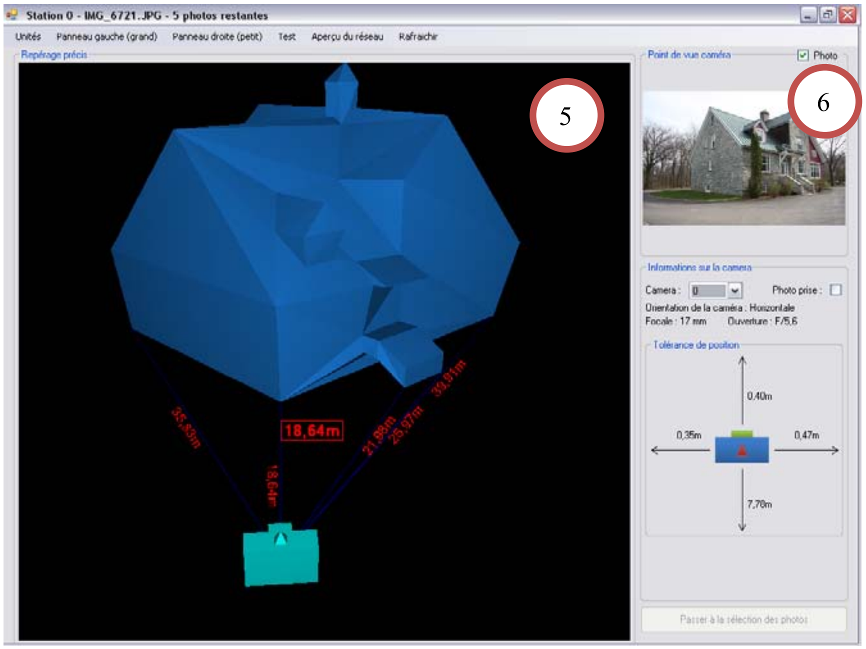

Station 0 - IMG_6721.JPG - 5 photos restantes

Repérage précis

Point de vue caméra ☑ Photo

Informations sur la camera

Camera : 0 Photo prise : □

Orientation de la caméra : Horizontale

Focale : 17 mm Ouverture : F/5,6

Tolérance de position

Figure 2. Other views available in the interface.

DESCRIPTION OF THE SIMULATOR

The main purpose of the simulator is to anticipate potential deviations in the precision of the final model due to erroneous or imprecise user manipulation during the photograph acquisition stage. As described in the introduction, the simulator is mainly dedicated to infrastructure monitoring process. As stated before, we assume the infrastructure under study has already been surveyed. Therefore a 3D model is already available.

The simulator uses, as input data, the infrastructure 3D model composed of 3D points and 3D surfaces, and the photogrammetric network, computed based on the original 3D model. More specifically, the network information that is imported in the simulator concerns the parameters associated with the interior and exterior orientation of each camera. These parameters are:

- The camera position: 3 unknowns (X_0, Y_0, Z_0)
- The camera orientation: 3 unknowns (ω, φ, κ)
- The principal point of auto-collimation: 2 unknowns (x_0, y_0)
- The focal length: 1 unknown (c)

As output data, the simulator provides information about points' precision and visibility, which are used to compute a "safe zone" in which the network requirements are fulfilled. The proposed simulator has been designed according to the following idea: since the simulator aims at assessing the loss of precision related to different photograph acquisition manipulations, its components should model the impact of these manipulations on the parameters involved in the 3D model computation. Two kinds of impact have been identified:

1. Erroneous manipulations can be modeled through the addition of bias values to the parameters specified by the previously-computed photogrammetric network: adding bias to the network parameters allows assessing the maximum deviations from the ideal values the photogrammetric process can accept in order to fulfill the expected precision. These deviations are related to the user imprecise manipulation (ex. imprecise position of a camera station).
2. The 3D modeling relies on the images acquired by the camera network. Relevant points characterizing the object under study are extracting from these images using Equation 2. So the 3D modeling process involves, on the one hand, camera configuration (position and orientation), and, on the other hand, image-coordinates of the extracted points. Although errors induced by this extraction processing result from an image processing algorithm rather than a user imprecise manipulation, they can still be modeled through the addition of noise to the image coordinates. More detail will be given in the description of the fourth component of the simulator (see below).

Thus, the workflow, displayed on Figure 3, has been designed in order to model the impacts of the user manipulations on the parameters involved in the 3D model computation. This workflow consists of the following components (also circled on Figure 3):

- Component 1: Data input: dedicated to loading the 3D model and the network setup into the system
- Component 2: Modeling of the parameters maximal deviation
- Component 3: 3D point projection, and occlusion handling
- Component 4: Modeling of the performance of the point extraction algorithm
- Component 5: Bundle block adjustment
- Component 6: Data output: information about the resulting model precision

Each of these components will be described in the following sections.

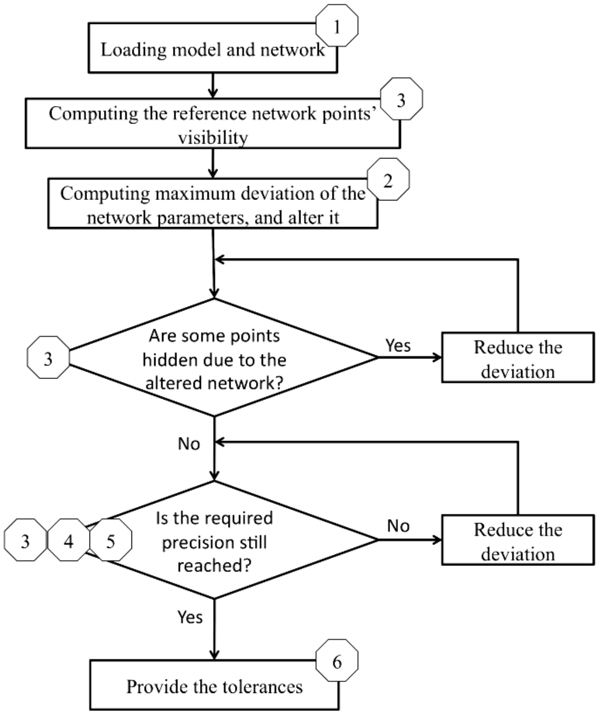

1
Loading model and network
3
Computing the reference network points' visibility
2
Computing maximum deviation of the network parameters, and alter it
3
Are some points hidden due to the altered network?
Yes
Reduce the deviation
No
3
4
5
Is the required precision still reached?
No
Reduce the deviation
Yes
6
Provide the tolerances

Figure 3. The simulator's workflow.

Model and Network Loading

The first component of the simulator aims at loading the infrastructure 3D model, and the network parameters. The 3D faces of the model will be used by the 3D point projection component (i.e. component 3) when checking the points' visibility. The triangle data structure has been chosen for the surface model representation since, generally, the surface of an infrastructure 3D model is a discrete surface, and the triangular modeling is a simple and widely used (e.g. DirectX, OpenGL) representation to conduct computations based on the model.

Parameters Maximum Deviation Modeling

This component aims at modeling the potential parameter deviations from the network specifications that could occur due to user inadequate manipulations. Therefore, typical user actions that could impact the resulting 3D model precision need to be replicated. As indicated in the previous section, the modeling of the deviations induced by the user inadequate manipulations is carried out through the addition of bias to the camera parameters, and more especially on the camera position along 4 axes:

- Along the camera-object axis: the acquisition station is positioned in front of the camera ideal position
- Along the camera-object axis: the acquisition station is positioned behind the camera ideal position
- Along the axis perpendicular to the camera-object axis: the acquisition station is positioned on the left side of the camera ideal position
- Along the axis perpendicular to the camera-object axis; the acquisition station is positioned on the right side of the camera ideal position

The object refers here to the infrastructure under study. The computation of the maximum deviation for each of the four axes quoted above is detailed below:

Maximum deviation computation when the acquisition station is positioned in front of the camera (Figure 4a); the maximum deviation is associated to the difference between the closest distance to the object, and the current distance to the object. The closest distance (distance 0-2''on Figure 4a) is considered here as the closest distance to the object for which all the points that were visible according to the viewpoint specified by the network setup are still visible. In other word, the maximum deviation computation consists in moving the camera forward toward the object until a point becomes hidden. The computation relies on simple trigonometric principles. In order to keep a security margin when computing the maximum deviation allowed, a smaller sensor size (red part on Figure 4a) is used.

Maximum deviation computation when the acquisition station is positioned behind the camera (Figure 4b); the maximum deviation is computed using the required monitoring precision (σ). Here we state that σ cannot be met if the size of a pixel projected on the object is greater than σ (which is not entirely true). This will occur if the user moves too far away from the object. So to compute the maximum deviation (d), we consider that the spatial resolution of the pixel equals σ if the camera is located at a distance d behind the camera. According to optics and trigonometry principles, the ratio of the spatial resolution by the focal length equals the ratio of σ by the distance d (i.e. 1pix/focal = σ/d). In order to keep a security margin when computing the maximum deviation allowed, the distance d value is divided at least by 2.

Maximum deviation computation when the acquisition station is positioned on the left and right sides of the camera (Figure 4c); the computation of these two deviations is based on the angle (α) from the original camera-3D model axis and the modified camera-3D model axis; this second axis is formed by the position of the camera at the modified location and the point aimed from the original location of the camera. The maximum deviation is computed using this angle. Indeed, a too high value for (α) could impact the convergence among the camera stations and as a consequence, the computation of the 3D model. Let's consider the distance (d') between the camera and the object. The deviation on the left or right of the camera is provided by the following trigonometric relationship: d' * tan (α). Knowing what is the maximum angle value that would warranty a suitable convergence among the camera stations, the maximum deviation can be determined.

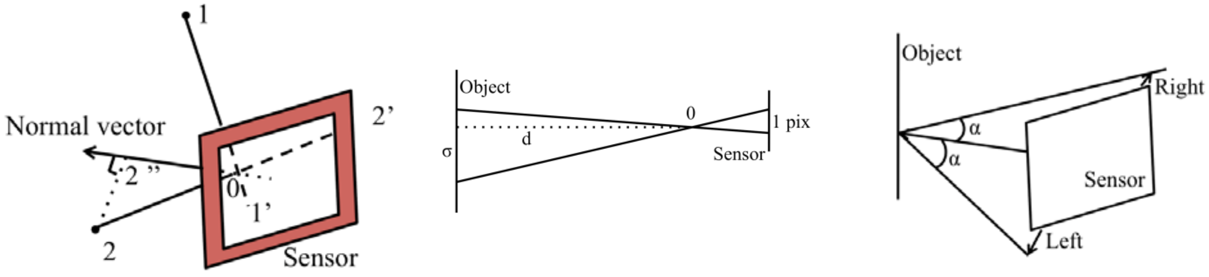

a) Front b) Back c) Left - Right

Figure 4. Deviations modeling.

Camera reorientation after change in location. To fully model the user behavior, the simulator reorients the camera angles in addition to translating the camera position. Indeed, as illustrated in Figure 5, any user will tend to aim at the object of interest after moving to a new location. If no reorientation is performed, the sensor's plane of the new location will be parallel to the sensor's plane of the camera initial position.

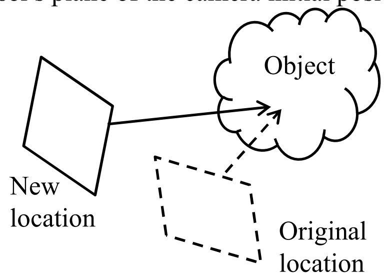

Figure 5. Orientation readjustment.

To compute the new camera angles after reorientation, the "*aiming vector"* has to be defined first. This vector is normal to the camera sensor plane and anchored to the camera position (X_0, Y_0, Z_0). The vector direction is opposite to the sensor's z-axis as shown in Figure 6, where (X, Y, Z) correspond to the ground coordinates system. The aiming vector is actually defined by two points: the camera position and a fictional aiming point, which can be arbitrarily chosen somewhere along the z-axis. In the proposed study, the aiming point is considered to be the same before and after camera reorientation. So its location is determined using the mean distance to all visible points' projection on the z-axis of the sensor (Figure 7), where *1* and *2* are 3D points belonging to the model.

The camera orientation angles cannot be determined based only on the knowledge of the aiming vector direction. Indeed, only 2 angles out of 3 (*ω*, *φ*) can be computed from this information. The roll angle around the sensor's z-axis (*κ*) is being unconstrained. To solve this problem, we choose to keep *κ* initial value (i.e. value before reorientation). Such simplification is considered acceptable since the roll angle is barely affected by the user manipulations when he tries to aim at the object of interest after moving to a new location.

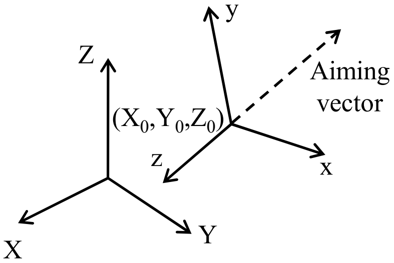

Figure 6. Aiming vector.

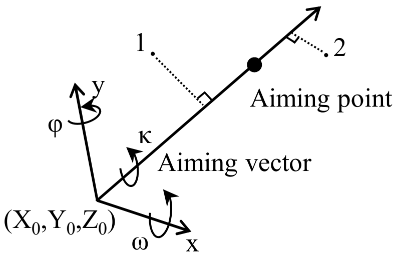

Figure 7. Aiming point.

3D Points Projection

This simulator component aims at projecting the 3D points of the model according to the different camera viewpoints, in order to get their image-coordinates with respect to the network setup. Shih (Shih, 1996) used the collinearity equations (Eq. 2) for such a purpose in his simulator. However he did not tackle the occlusion problem. To address this issue, the proposed simulator combines Shih's approach with a visibility algorithm. Figure 9 presents the main steps of this algorithm. The model 3D points are projected onto the images acquired at each camera station. The visibility algorithm's role is to check if the 3D points are visible from the selected viewpoint. To be visible, a point must satisfy two conditions:

1. Its image-coordinates must be in the picture area;
2. It must not be occluded by any triangular face of the model.

The occlusion algorithm used here is based on tetrahedron volume difference. This method has been developed since the volume of a tetrahedron can be directly computed based on its vertices 3D coordinates, if its apex is at the origin of the coordinate system (Eq. 1). Therefore this approach is not time consuming.

$$V = X_1 * (Y_2 * Z_3 - Z_2 * Y_3) + Y_1 * (Z_2 * X_3 - X_2 * Z_3) + Z_1 * (X_2 * Y_3 - Y_2 * X_3) \qquad \text{Eq. 1}$$

The occlusion algorithm can be split into 4 distinct cases as illustrated in Figure 8. The camera (viewpoint) is noted Vp, the point whose visibility is checked is noted P. The triangle three vertices are noted respectively 1, 2, 3.

Let's name the following tetrahedron's volumes:

- $V_1 = V_{Vp\text{-}P\text{-}2\text{-}3}$
- $V_2 = V_{Vp\text{-}P\text{-}1\text{-}3}$
- $V_3 = V_{Vp\text{-}P\text{-}1\text{-}2}$
- $V_T = V_{Vp\text{-}1\text{-}2\text{-}3}$
- $V_P = V_{P\text{-}1\text{-}2\text{-}3}$

According to Figure 8, only 1 case involves a context where point P is hidden. The corresponding volume computation equation is the following: $V_1+V_2+V_3=V_T+V_P$. So for each triangle, if this equation is not true, the point is visible, otherwise, it is hidden.

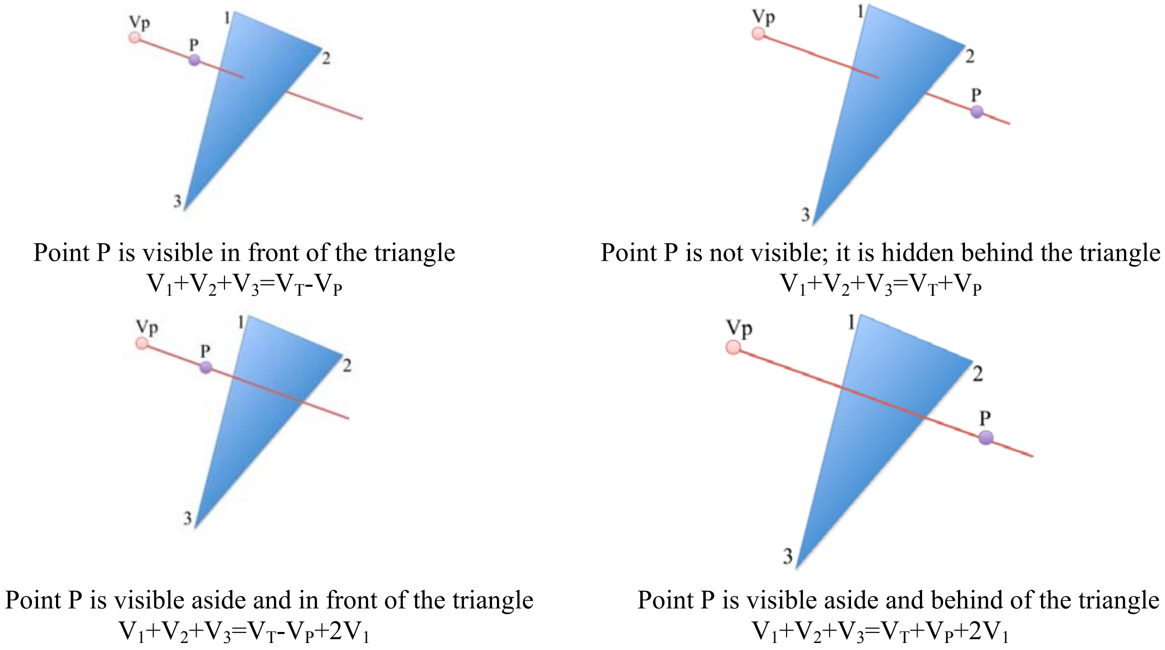

Point P is visible in front of the triangle
$V_1+V_2+V_3=V_T-V_P$

Point P is not visible; it is hidden behind the triangle
$V_1+V_2+V_3=V_T+V_P$

Point P is visible aside and in front of the triangle
$V_1+V_2+V_3=V_T-V_P+2V_1$

Point P is visible aside and behind of the triangle
$V_1+V_2+V_3=V_T+V_P+2V_1$

Figure 8. The 4 cases addressed by the occlusion algorithm.

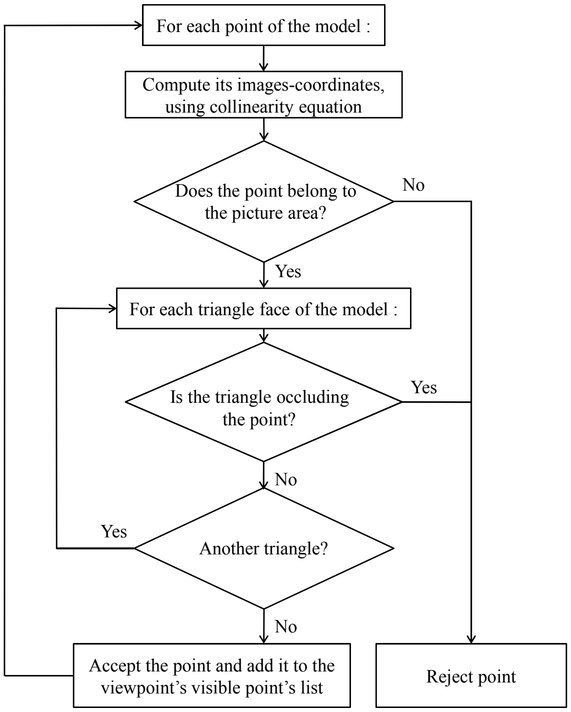
For each point of the model :
Compute its images-coordinates, using collinearity equation
Does the point belong to the picture area?
No
Yes
For each triangle face of the model :
Is the triangle occluding the point?
Yes
No
Another triangle?
Yes
No
Accept the point and add it to the viewpoint's visible point's list
Reject point

Figure 9. Visibility algorithm.

Modeling of the Point Extraction Algorithm Performance

An incorrect or imprecise user manipulation during the acquisition phase is not the only source of inaccuracy in the course of the 3D modeling process. Imprecision can also stems from the 3D point selection on the pictures. Contrary to the simulation mode where the theoretical image-coordinates of the points are computed using equation

(Eq. 2), usual 3D modeling requires to extract manually these coordinates directly on the pictures or to use a feature extraction algorithm. Therefore this imprecision source has to be simulated as well. This is achieved once the projection process has been completed. The image-coordinates of the 3D points are computed in pixel unit with double precision (15 to 16 digits). Such precision involves coordinate values with 11 to 12 decimals. These are the exact theoretical coordinates of the point. However, when a user or a feature detection algorithm extracts these coordinates, their value involved generally 2 decimals precision at best. Therefore, the coordinates of the 3D points have to be rounded to a reasonable number of decimals to reflect the usual inaccuracy of the data extraction process. Such rounding operation is also performed after having projected the points according to the original network configuration. This operation is essential to know the theoretical precision reached by the initial network. If omitted, each of the image-coordinates would be so accurate that the residuals of the bundle block adjustment would be equal to zero.

To further simulate the inaccuracy of the 3D point extraction on the pictures (either by the user or by an image processing algorithm), Gaussian noise can be added to their images-coordinates. Adding noise is similar as, for example, extracting 3D point coordinates with a point precision of ±1 pixel on the picture.

$$
\begin{aligned}
x' &= x'_0 - c\frac{r_{11}(X-X_0)+r_{21}(Y-Y_0)+r_{31}(Z-Z_0)}{r_{13}(X-X_0)+r_{23}(Y-Y_0)+r_{33}(Z-Z_0)} \\
y' &= y'_0 - c\frac{r_{12}(X-X_0)+r_{22}(Y-Y_0)+r_{32}(Z-Z_0)}{r_{13}(X-X_0)+r_{23}(Y-Y_0)+r_{33}(Z-Z_0)}
\end{aligned}
\qquad \text{Eq. 2}
$$

Bundle Block Adjustment of the Model

The bundle block adjustment component allows computing the resulting 3D model associated to the new network setup. Reduced normal equations technique, as expressed by Kraus (Kraus, 1993), has been used in this study to compute the adjustments.

The simulator is designed to adjust up to 9 parameters per viewpoint (cf. the overview of the simulator), and 3 parameters per unknown points (3D coordinates). All these parameters can be freely fixed on demand, but it would be more relevant to fix only the parameters on which noise has been added in the previous steps. Otherwise the bias will be adjusted during computation. For example, if a bias is added on the camera position, the camera coordinates must be fixed in order to assess the precision deviation due to the bias. Most of the time, the viewpoints' parameters are fixed, and the only unknowns are the 3D coordinates of the model points.

Assessment of the Resulting 3D Model Precision

After the bundle block adjustment step, the simulator outputs information about the parameters yielded by the bundle block adjustment computation. The information is the following:

- The standard error of unit of weight (σ_0) or standard deviation of image-coordinates: this is an important indicator of the overall precision of the least square adjustment
- The standard deviation of ground-coordinates of each points of the model, with the network parameters set as fixed values (not adjusted)
- The precision of each parameter of the network that has been set as being tunable

These parameters can be compared to those from the original setup of the network in order to detect some precision loss.

All these results may not be very informative to a non-expert user when displayed as raw numbers. So in order to translate them into meaningful recommendations to the user, these outputs are used to set the tolerances on the camera position. When every standard deviation for each of the coordinates of all the 3D points are below the required precision, the simulator returns a positive validation of the acquisition configuration as the result of its analysis.

RESULTS WITH TEST USERS

A test session has been conducted on site involving three people (a geographer, and two civil engineers). The tests consisted for them to take pictures of a building while following the instructions of the proposed solution. The equipment used was a Canon SLR Digital Rebel XT, a non-metric camera with an 8 Megapixels sensor. The lens' focal length was 17-85mm with optical stabilization. The proposed solution has been implemented on a Tablet PC, running under Windows XP for Tablet PC, with a 1.5 GHz dual core, no graphic acceleration and 2Go of RAM. The purpose of these tests was to validate the adequacy of the proposed guiding tool and underline possible usage problems. In addition, they aimed at assessing the precision these users could achieved in relation to the reference network.

The users were invited to go on site with the equipment, and take pictures according to the information displayed on the Tablet PC (Figure 10). The instructor was standing next to them to observe, write comments about their usage of the solution and sometimes give some direct instruction depending on the user's behavior, usually to be sure the user understands correctly the information provided.

The following table synthesizes the test result.

Table 1

User	Geographer	Civil engineer 1	Civil engineer 2
Remarks / behavior	• Distances are assessed with difficulties • Uses a lot the displayed distances to position the camera station • Navigates easily in the interface	• Tries to replicate the original picture • Navigates easily in the interface • Takes a lot of bearings	• Needs the measures in feet • Needs to see the center of images • Takes into account the tolerances
Max deviation from the reference network	8m	2m	2m

Figure 10. People testing the solution.

User tests helped demonstrate the global relevance and adequacy of the proposed solution from an usage standpoint. The tolerances given by the simulator were sometimes very constraining. Nonetheless the users managed to go through the acquisition process while meeting these constraining. Over the whole test series, most of the pictures were taken within the tolerances. But, as suggested by the users, a portable distance measurement device could help them verify how far they stand from the object under study. Concerning the usability of the interface, the users got acquainted quickly with the proposed solution. After few minutes of manipulation, they managed to find their way through the interface and get the information they required for the acquisition process.

CONCLUSION

This paper presented the solution we proposed to assist non-expert users through on site data acquisition process towards the 3D modeling of infrastructure. This solution is composed of an interactive interface providing the user with an overview as well as a detailed representation of the acquisition context. The solution consists of a simulator too which is dedicated to the impact estimation of user incorrect picture acquisition on the resulting 3D model accuracy. This component provides tolerance values regarding the acquisition stations compared to the theoretical camera positions. The various components involved in the simulator design have been fully detailed in the paper. Specific contributions of the proposed approach concern the modeling of the deviations induced by the user inadequate manipulations and the visibility algorithm involved in the 3D point projection component. Feedbacks from the users have been greatly positive, and their results are very encouraging. Since the network design module is not complete yet, the reference network used for the test has not been established through a computational process but by an expert in photogrammetry. Such an approach is not ideal for our case, because an algorithm can provide a network configuration using various constraints (e.g. having the same tolerance on the left and on the right of the camera), while a human can only process by iterations. Future work will be dedicated to the implementation of a new version of the proposed solution according to the user comments. In addition, a new module dedicated to checking the pictures validity on site will be developed. This module will involve image correlation or model tracking algorithms.

REFERENCES

Brown, J., 1997. V-STARS / S Acceptance Test Results, *Geodetic system Inc.* [Online] http://www.geodetic.com/Downloadfiles/S Acceptance Test Results metric version.pdf.

Chandler, J., 1999. Effective application of automated digital photogrammetry for geomorphological research, *Earth Surface Processes and Landforms*, Vol. 24, 1, pp. 51-63.

Drap, P., P. Grussenmeyer, AND G. Gaillard, 2001. Simple photogrammetric methods with arpenteur 3-D plotting and orthoimage generation: the I-MAGE process, *International Archives of Photogrammetry Remote Sensing and Spatial Information Sciences*, Vol. 34, 5/C7, pp. 47-54.

Kraus, K., 1993. *Photogrammetry : Fundamentals and Standard Processes,* Ferd. Dümmlers Verlag, Vol. 1.

Marzolff, I., AND J. Poesen, 2009. The potential of 3D gully monitoring with GIS using high-resolution aerial photography and a digital photogrammetry system, *Geomorphology*, Vol. 111, 1-2, pp. 48-60.

Remondino, F., AND S. El-Hakim, 2006. Image-based 3D modelling: a review, *The Photogrammetric Record,* Vol. 21, 115, pp. 269-291.

Shih, T.Y., 1996. A photogrammetric Simulator for close-fange application, *Photogrammetric Engineering & Remote Sensing*, Vol. 62, 1, pp. 89-92.

Walker, J.P., and G.R.Willgoose, 1999. On the effect of digital elevation model accuracy on hydrology and geomorphology, *Water Resources Research*, Vol. 35, 7, pp. 2259-2268.